Optic cavitation with CW lasers: A review

J. P. Padilla-Martinez, C. Berrospe-Rodriguez, G. Aguilar, J. C. Ramirez-San-Juan, and R. Ramos-Garcia

Citation: Physics of Fluids **26**, 122007 (2014); doi: 10.1063/1.4904718
View online: http://dx.doi.org/10.1063/1.4904718
View Table of Contents: http://scitation.aip.org/content/aip/journal/pof2/26/12?ver=pdfcov
Published by the AIP Publishing

PHYSICS OF FLUIDS **26**, 122007 (2014)

Optic cavitation with CW lasers: A review

J. P. Padilla-Martinez,[1] C. Berrospe-Rodriguez,[1] G. Aguilar,[2]
J. C. Ramirez-San-Juan,[1] and R. Ramos-Garcia[1,a)]
[1]*Departamento de Óptica, Instituto Nacional de Astrofísica, Óptica y Electrónica, Puebla 72000, México*
[2]*Department of Mechanical Engineering, University of California Riverside, Riverside, California 92521, USA*

(Received 27 May 2014; accepted 4 November 2014; published online 23 December 2014)

The most common method to generate optic cavitation involves the focusing of short-pulsed lasers in a transparent liquid media. In this work, we review a novel method of optic cavitation that uses low power CW lasers incident in highly absorbing liquids. This novel method of cavitation is called thermocavitation. Light absorbed heats up the liquid beyond its boiling temperature (spinodal limit) in a time span of microseconds to milliseconds (depending on the optical intensity). Once the liquid is heated up to its spinodal limit (~300 °C for pure water), the superheated water becomes unstable to random density fluctuations and an explosive phase transition to vapor takes place producing a fast-expanding vapor bubble. Eventually, the bubble collapses emitting a strong shock-wave. The bubble is always attached to the surface taking a semi-spherical shape, in contrast to that produced by pulsed lasers in transparent liquids, where the bubble is produced at the focal point. Using high speed video (10^5 frames/s), we study the bubble's dynamic behavior. Finally, we show that heat diffusion determines the water superheated volume and, therefore, the amplitude of the shock wave. A full experimental characterization of thermocavitation is described. [http://dx.doi.org/10.1063/1.4904718]

I. INTRODUCTION

Research in cavitation bubble dynamics near a solid wall was mainly motivated by the urge to understand the destructive action of bubbles on solid surfaces, in particular on the propeller blades of fast steamships.[1] The first analytical study of cavitation and its dynamics was made by Rayleigh.[2] Since then, a great deal of work describing cavitation bubbles has been published and compiled in several books[3–5] providing a good understanding of the physics of bubble dynamics. Cavitation bubble's collapse is responsible for a number of interesting phenomena including: luminescence,[6] ultrasound generation,[7] damage to surfaces,[8] surface cleaning,[9] and medical applications such as lithotripsy[10,11] among others.

The most common methods to produce cavitation bubbles include: (i) the use of ultrasound generated by piezoelectric transducers (*acoustic cavitation*),[11–13] which is widely used in medical applications; (ii) high speed water flow like those obtained in propellers or hydraulic machinery (*hydraulic cavitation*);[14] (iii) electric discharge or elementary particles in water (*particle cavitation*);[15] and (iv) lasers focused into low absorption coefficient solutions (*optical cavitation:* OC).[8,9,16–20] In this work, we will center our attention on OC, especially in cavitation produced by continuous wavelength lasers as opposed to OC produced by short-pulsed lasers (SPL), where nonlinear light absorption and/or cascading ionization produce a hot and supersonic expanding plasma bubble which, upon collapse, generates shockwaves of several GPa of pressure amplitude. OC by SLP has been extensively studied over the last 2-3 decades and, for such a reason, it will not be discussed in this work.[8,9,16–20]

a)Author to whom correspondence should be addressed. Electronic mail: rgarcia@inaoep.mx

Thermocavitation produced by CW lasers, was first reported by Rastopov and Sukhodolsky back in 1992,[21,22] but has been largely neglected partially due to the research boom in OC by SPL. Thermocavitation is quite attractive due to its experimental simplicity and low cost. The physical mechanism of cavitation outlined by Rastopov and Sukhodolsky[21,22] is the creation of an overheated region (~300 °C) at the focal point, followed by an explosive liquid-vapor phase transition. The superheated vapor increases its volume by many orders of magnitude as compared to liquid, producing in this way a fast expanding vapor bubble. In thermocavitation, no plasma is created due to the relative low intensity of the laser. Thus, the physical mechanism is quite different to that produced by SLP; the heating limit of water is determined by the spinodal (~300 °C) temperature of water and not by the plasma, which can reach up to several thousand degrees.[19] Thermocavitation was later studied indirectly by other research groups interested in ablation of biological materials using the relative high absorption coefficient of water and biological tissue in the wavelength range of 2-3 μm.[23,24] In particular, Ho:YAG laser (λ = 2.1 μm) and Er:YSGG laser (λ = 2.79 μm) have been used for efficient tissue ablation in urology in order to fragment stones or calculi from the urinary tract, i.e., kidney, bladder, or urethra.[25] Finally, it was noticed that at the output end of optical fibers covered with nanoparticles immersed in water, vapor bubbles were formed due to heat transfer from the nanoparticles to the water.[26] If sufficient power is transmitted through the fiber, then shock waves are produced.[27] In fact, many of the conclusions presented in this paper were also outlined in the aforementioned papers, but thermocavitation was not recognized as a new cavitation method in its own right. In this review, the physical mechanism of thermocavitation is discussed and a full characterization of thermocavitation for optimal bubble size and shock wave amplitude is reported.

II. EXPERIMENTAL DESCRIPTION

The optical set up for cavitation bubbles generation is quite simple; a collimated CW laser beam (λ = 975 nm) is focused on a glass cuvette containing a highly absorbing solution. We use a microscope objective (f = 8 mm) in an inverted microscope configuration to produce a spot of ~2 μm diameter at the focal point (Figure 1). The focal point is placed on the cuvette's inner surface, i.e., the glass-solution interface. This position is identified as the reference level $z = 0$. Since the microscope objective is mounted on a translation stage, the position of the focal point inside the cuvette can be manually controlled either inside the solution ($z > 0$) or inside the glass ($z < 0$). This allows control of the beam spot size, which is an important parameter in thermocavitation, as discussed

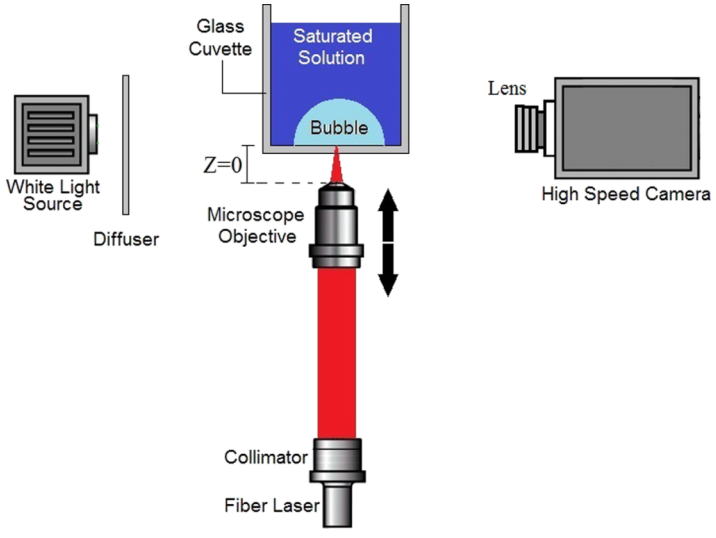

FIG. 1. Experimental setup used for the generation and analysis of vapor bubbles. The lens with f = 12.7 cm is used to image the bubble into the CCD camera. A hydrophone (not shown) is used to measure the amplitude of the shockwaves.

below. The cuvette is filled with a saturated solution of copper nitrate ($CuNO_4$) dissolved in water (13.78 g of $CuNO_4$ per 10 ml of water) at room temperature. The absorption coefficient of the solution, α (135 cm^{-1}) is so large at this laser wavelength that light is strongly absorbed near the cuvette-solution interface (penetration depth ~74 μm). In order to record the formation and evolution of an individual bubble, the cuvette is illuminated perpendicular to the laser beam direction with a white light source, and imaged with a high speed video camera (Phantom V7, Version: 9.1 frame rate of 10^5 frames/s). The laser's current is externally modulated to produce pulses of the desired length in order to control the number of cavitation events. A hydrophone (HP) is placed inside the solution to measure the amplitude of the shockwave produced upon collapse of the bubbles. The hydrophone is connected to a recording digital oscilloscope. It is important to point out that thermocavitation can be obtained in any solution as long as the absorption coefficient at the illumination wavelength is large. For example, Rhodamine-doped water can be used for green light (λ = 532 nm),[21] toner microparticles or carbon nanotubes dissolved in water strongly absorb visible light.[28] We chose $CuNO_4$ because it strongly absorbs NIR (λ = 975 nm) radiation and does not degrade as organic dyes do.

III. RESULTS

Figure 2 shows the typical temporal evolution of a single cavitation bubble created with a 150 mW power laser focused inside the solution ($z \sim 260$ μm). These conditions produce the largest bubbles in our experiment. Later on, we will discuss on how to optimize bubble radius and shockwave amplitude emission upon collapse. One distinctive characteristic of thermocavitation is that vapor bubbles are always in contact with the substrate taking a semi-spherical shape regardless of the position of the beam focal point inside (or outside) the solution (Figures 2(a) and 2(b)). Due to the short light penetration depth (~74 μm), changing the position of the focal point only changes the volume of the superheated volume and, therefore, the size of the bubble and amplitude of the emitted shockwave.[7,29] In contrast, bubbles created with short pulsed lasers in transparent solutions are always produced at the focal point where the intensity is the highest. The left-most image in Figure 2(a) corresponds to the shadow produced just before vapor bubble formation. The dark region of approximately 150 μm height and 100 μm wide is produced by light refraction on the superheated water. Note that due to heat diffusion, this region is much larger than the physical dimensions of the beam (2 μm at the glass-solution interface and 40 μm at z = 260 μm above the interface taking a Rayleigh distance of ~13 μm).

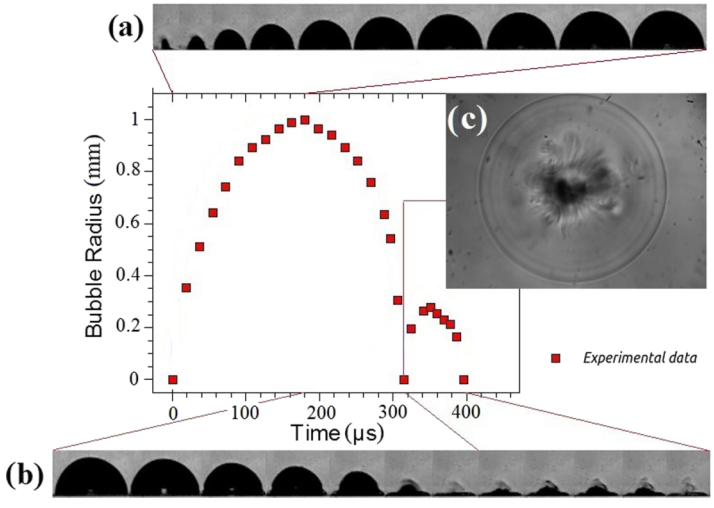

FIG. 2. Temporal evolution of a single bubble formed at $z \sim 260$ μm and $I \sim 0.7$ kW/cm^2. Side-view (a) expanding bubble, (b) bubble collapse and rebound, and (c) top-viewed of the bubble collapse and shock wave emission. (Multimedia view) [URL: http://dx.doi.org/10.1063/1.4904718.1]

Once the bubble is generated, it grows regularly without any significant modification to its half-hemisphere shape, reaches its maximum radius $R_{max} \sim 1$ mm in 180 μs (Figure 2(a) Multimedia view) and then it collapses in just 135 μs (Figure 2(b)). At this moment, a shockwave is emitted as demonstrated in Ref. 30. The emission of the shockwave is not visible in Figures 2(a) and 2(b) because of the limited time resolution of the camera (10 μs). The speed of the sound in the solution is 1800 m/s, or 18 mm in 10 μs, which is well above the field of view (FOV) of the optical system of 2×1 mm^2. Therefore, to obtain a partial view of the shock wave, a second high speed image sequence was obtained from the top, where the FOV could be increased to 20×10 mm^2. The circle around the dark area in Figure 2(c) shows the shockwave produced ~10 μs after the collapse of one bubble. It is important to mention that electronic synchronization is quite difficult due to jitter (as discussed below). In the bubble radius time sequence of Figure 2(b), it is possible to observe a slight rebound with duration of 81 μs, whose radius is five times smaller than R_{max}. Contrary to Rastopov and Sukhodolsky,[21,22] we found that the rebound bubble radius is always smaller than R_{max}. This is easy to understand since, in the first collapse, most of the kinetic energy is released in the form of mechanical energy (shock waves).

The fact that only one rebound is observed in our experiments indicates that the bubble collapse is strongly damped. As reported before, a strong shock wave is emitted upon collapse, whose amplitude scales linearly with the bubble radius.[30] In fact, Vogel *et al.*,[31] found that for laser-induced pulsed cavitation, up to 70%-90% of the input energy is converted into mechanical energy. Although these results are valid for pulsed illumination in pure water, acoustic losses also dominate in thermocavitation. In fact, the amount of energy lost by the bubble depicted in Figure 1 is calculated to be ~80% according to the analysis of Ref. 31. This is consistent with the theoretical model of Fujikawa and Akamatsu,[32] which includes the effects of compressibility of the liquid, non-equilibrium condensation of the vapour, heat conduction, temperature discontinuity at the phase interface, and the emission of shock waves. The presence of a solid boundary has shown to greatly affect the bubble shape and dynamics, for example, bubble collapse may produce water jets aimed towards the substrate.[1,2,8,9,18] However, this effect was not clearly distinguished in thermocavitation where the proximity factor γ ($=l/R_{max}$, where l is the distance from the substrate to the bubble center and R_{max} is the maximum bubble radius) is zero, at least at the maximum time resolution of our imaging system (10 μs). It is worth mentioning, that friction with the substrate slightly affects the shape of the bubble, particularly on the final stage of collapse, and it is not clear how this apparently small effect could affect its dynamics. It is evident that further studies with higher temporal resolution are needed to analyze the bubble dynamics near the collapse, but these studies are beyond the scope of this paper.

Thermocavitation is not a single-event phenomenon; in fact, it is a multi-event and supposedly a periodic process.[22] Figure 3 shows the frequency and amplitude of the shockwave as function of

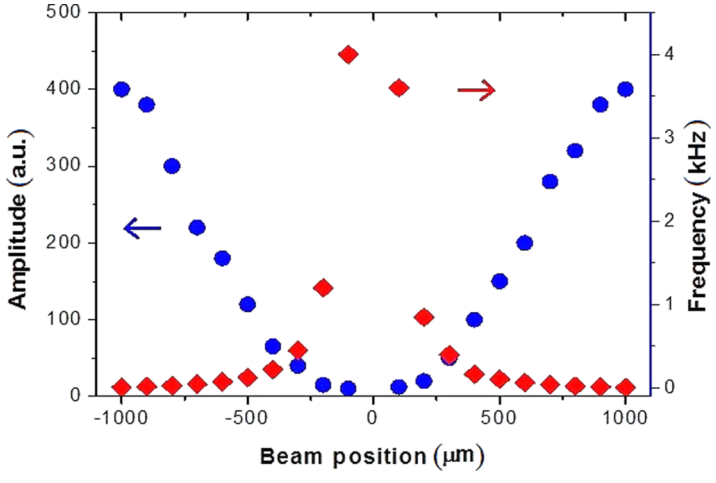

FIG. 3. Frequency (♦) and amplitude (●) of the emitted shockwave under CW laser illumination.

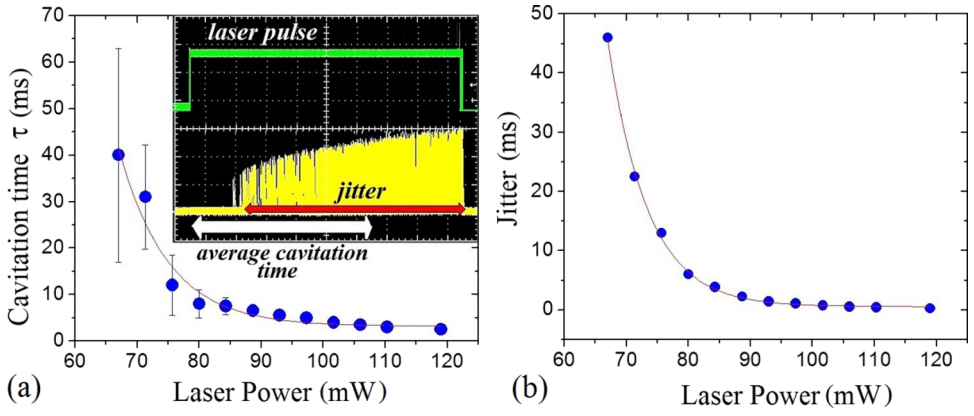

FIG. 4. (a) Cavitation time behavior as a function of laser power. (●) Experimental data and the error bars represent the fluctuations on time (jitter). (b) Exponential decay of jitter as a function of laser power. Continuous line is fit to an exponential function.

the beam focus position ($z = 0$ is the glass-solution interface) for a power of 120 mW. Each point represents an average of 20 events. The frequency and amplitude were measured with a hydrophone and the signal displayed on a digital oscilloscope; more experimental details can be found in Ref. 30. The first striking feature is that the shockwave amplitude is larger when the beam is focused well above or below the glass-solution interface but the cavitation frequency is quite small. On the other hand, near the focus, the frequency is quite high (~4 kHz) but the amplitude is rather small.

It was also found that cavitation generation rate is not periodic but it rather shows a quasi-periodic behavior, with jitter being much larger at low power and decreases as power increases, as shown in Figure 4. In order to measure both the cavitation rate and jitter, the laser current was temporally modulated to generate 250 single-cavitation events. The oscilloscope was used in persistence mode in order to observe all generated signals simultaneously on a single screen. The laser was focused at the glass-solution interface ($z = 0$); results for $z \neq 0$ are basically the same but obviously the cavitation rate and jitter are of different values. It is important to mention that heating up to the spinodal limit (or cavitation temperature) is not instantaneous, the time to reach it is called thermocavitation time τ (Ref. 30). The inset picture in Figure 4(a) shows the typical signals that were monitored: (i) laser pulse (green line) and (ii) HP signal (yellow line); each vertical line corresponds to a single cavitation event for 67 mW of laser power. During a single laser pulse, a single cavitation event occurs but neither the cavitation time nor the amplitude of the emitted shock wave is of the same magnitude. The white arrow represents the average cavitation time, while the red arrow represents the span in cavitation time (*jitter*). The cavitation time may occur ~15 ms after the laser has been turned on, or up to 62 ms later. This variation in cavitation time makes difficult the synchronization of the different electric signals. Note that the latest the cavitation event, the larger its amplitude; this makes sense since the later the event, the more energy is being deposited and thus the superheated volume is larger. Figure 4(a) shows the cavitation time as a function of laser power. The first point in the curve represents the threshold power for thermocavitation (67 mW), obtaining an average cavitation time $\tau = 40$ ms and a jitter of about 46 ms (error bar). When the power increases, the cavitation time decayed exponentially reaching a value around 2.5 ms for a power of 119 mW and jitter ~0.24 ms. Figure 4(b) shows the fluctuations on time (jitter) as a function of laser power.

For many applications such as surface damage[33] and ultrasound generation,[7] it is desirable to obtain the largest bubble possible. As mentioned earlier, this can be achieved by increasing the spot size in order to increase the superheated volume. However, if the spot is too large (for example, by focusing the beam far from $z = 0$) the intensity may drop below the threshold to generate cavitation. In such a case, the beam power must be increased. Figure 5(a) shows the maximum bubble radius (R_{max}) and the bubble lifetime reached when the laser focus is placed at $z \sim 35$ μm. The first data point corresponds again to the threshold intensity for bubble's formation $I_{Thr} \sim 16\,\mathrm{kW/cm^2}$ (P = 67 mW and ~22 μm spot diameter). This leads to a maximum bubble's radius of $R_{max} \sim 470$ μm with $\tau \sim 40$ ms

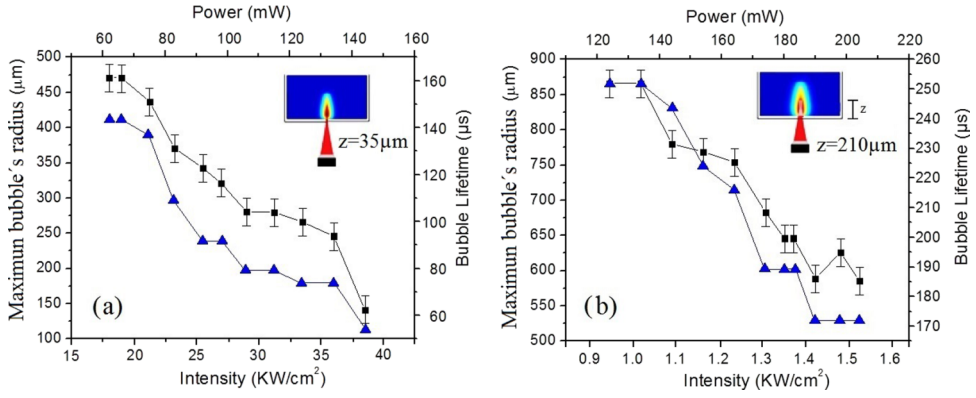

FIG. 5. (a) The laser focus was placed $z = 35\ \mu$m and (b) $z = 210\ \mu$m. (■) Maximum bubble's radius and (▲) bubble lifetime at different intensities.

and lifetime about 144 μs. As power is increased, both R_{max} and the bubble lifetime decrease almost linearly, at least in this power range. In previous works,[30] we showed that the reduction in bubble radius scales exponentially. Although the experimental conditions are different herein, there is no physical reason why this dependence should be different. In Figure 5(b), the laser focus was placed $z = 210\ \mu$m inside the sample (~130 μm spot diameter). We see a similar pattern to that shown in Figure 5(a). Note that the threshold intensity to generate cavitation decreases to ~0.92 kW/cm^2 (124 mW). Measurements report that the bubble lifetime $\tau_b \sim 252\ \mu$s and the maximum bubble radius increases to ~866 μm. Thus, if one is interested in obtaining maximum bubble's radius, one must use the largest possible spot at the glass-liquid interface while reaching the threshold intensity.

IV. DISCUSSION: PHYSICAL MECHANISM OF OPTIC CAVITATION

As mentioned already, in thermocavitation, light absorption and subsequent water heating play a critical role to produce vapor bubbles. Let us analyze the phase diagram of water and learn what happens when water is heated up. Figure 6 shows the phase diagram of water as pressure P *vs* temperature T for a specific volume V. The letters indicate the state of the substance at different conditions. For example, A represents the triple point at which the solid, liquid, and vapor states coexist. From this

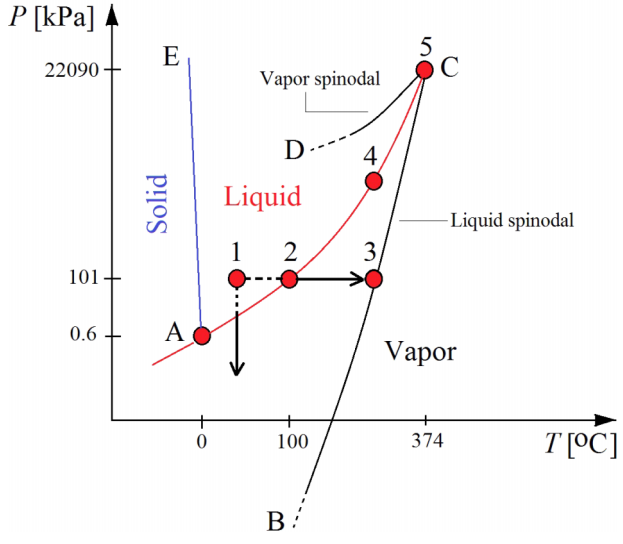

FIG. 6. Phase diagram for water at different temperatures and pressures.

point, it is possible to obtain the solid phase by increasing the pressure and decreasing the temperature; alternatively, if the pressure and temperature increase the liquid phase exists. The line AC represents the saturated liquid/vapor or *binodal line*. The curve BCD is the *spinodal* line which represents a locus of states representing the intrinsic stability limit of the liquid or vapor phase. The line CD is called the *vapor spinodal line*, and represents the limit to which metastable vapor can be subcooled; the line BC is called the *liquid spinodal line*, and represents the limit to which metastable liquids can be superheated. Clearly both spinodal lines end at the critical point C, above which no thermodynamic distinction can be made between liquid and vapor phases.[4,34]

The critical point conditions for water are $T_C = 374.14\,^{\circ}\text{C}$ at $P_C = 22.09$ MPa. In the same figure, additional points of interest have been labeled: Point 1 represents ambient conditions ($T_1 = 25\,^{\circ}\text{C}$ and $P_1 = 101$ kPa); point 2 denotes saturated liquid at atmospheric pressure, i.e., the "*boiling temperature*" ($T_2 = 100\,^{\circ}\text{C}$ and $P_2 = 101$ kPa); point 3 is the location of the spinodal line at ambient pressure ($T_3 = 305\,^{\circ}\text{C}$ and $P_3 = 101$ kPa).[34] This last point is of critical importance to understand thermocavitation. One normally thinks of cavitation as a reduction of ambient pressure (acoustic or hydraulic cavitation) at constant temperature, however, heating above the boiling temperature without actually boiling also leads to cavitation. This occurs because, even though the water is hot enough to boil, the surface tension of the liquid suppresses the formation of bubbles. For vapor bubbles to form and expand, the temperature of the liquid needs to be high enough that the vapor pressure of the liquid exceeds the vapor pressure of the ambient pressure. Superheating can be achieved in pure solutions (homogeneous nucleation) in containers with very smooth walls. Thus, the upper limit for superheating is determined by the liquid spinodal, i.e., 305 °C.[35] Once this temperature is reached, the liquid becomes highly unstable to perturbations and an explosive phase transition is achieved, generating a fast expanding bubble that eventually collapses.

The spinodal (~305 °C) is achieved under very special conditions like ultrapure water in oil (to reduce nucleation sites), otherwise the explosive phase transition may occur at temperatures < 305 °C. Different techniques have been implemented in order to measure the spinodal limit through cavitation, i.e., when the liquid reaches the spinodal, a violent liquid-vapor phase transition occurs. This temperature is often called as cavitation temperature T_{cav}. For example, the first attempt to measure it was reported by De Luc,[36] who heated water up in a glass flask in an oil bath and heated water up to 122.5 °C at atmospheric pressure without boiling. Refinements to the technique, in order to minimize the effect of impurities and to allow a quick thermalization, involve the use of small capillaries. Kenrick[37] found that the vapor explosion occurred at a maximum $T_{cav} = 270\,^{\circ}\text{C}$; this was later confirmed by Briggs.[38]

Droplets of water can be heated up in another liquid with higher boiling temperature.[39] This method involves a smooth liquid–liquid interface. At the bottom of a column of the host, a denser liquid temperature gradient is maintained and a droplet of liquid is injected. The droplet raises slowly and warms up until it cavitates at some height where T_{cav} is measured.[40,41] For water heated in silicone oil at atmospheric pressure, T_{cav} lies in the range of 250–280 °C.[42,43] Apfel achieved a maximum T_{cav} of 279.5 °C,[44] using silicone oil with benzyl benzoate. The liquid can also be directly heated by a thin platinum wire. A large current is passed through the heater for a short time (~10 μs). When a bubble nucleates, the wire reduces the heat transfer to the fluid, and the heater temperature raises. The corresponding change in resistance of the wire indicates cavitation; preliminary calibration of the resistance gives T_{cav}. Skripov obtained $T_{cav} = 302\,^{\circ}\text{C}$ (Ref. 45) at atmospheric pressure and was later confirmed by Derewnicki[46] and Glod,[47] obtaining $T_{cav} = 292$ and 303 °C, respectively, ±5 °C.[48] This value is close to the prediction of Classical Nucleation Theory (CNT) for homogeneous nucleation.[48,49] This method has been recently revisited by a number of groups using a thin film heater instead of a wire, and the maximum values of T_{cav} are similar. Using CO_2 lasers, where radiation is strongly absorbed by water, also allows determination of T_{cav}, giving $T_{cav} \sim 300\,^{\circ}\text{C}$ (Table I).[50,51]

With this information in hand, we can already highlight two main differences between short-pulsed cavitation and thermocavitation: (i) In short pulse cavitation, a hot (several thousand degrees centigrade) plasma is expanding after illumination while in thermocavitation, a superheated water vapor is expanding. (ii) In the latter case, there is an upper limit to the water vapor temperature, while in the former its temperature is determined by the pulse energy.

TABLE I. The observed superheated limit obtained for the water, using the different methods explained above.

Researcher	Method	T_{cav} (°C) at atmospheric pressure	References
Pinnick and Kudryashov	Laser induced cavitation	Above 300	50 and 51
Yavas		200	52
Dufour	Heating in a host liquid	178	39
Moore			
Wakeshima			
Blander			
Apfel		250 to 280	40–44
Skripov	Heat pulse	302	45
Derewnicki		292	46
Glod		303	47
De Luc	Heating in a capillary	122.5	36
Donny		135	53
Kenrick and Briggs		270	37 and 38
Brereton		240	54

V. NUCLEATION THEORY

CNT has been developed in several works;[48,49] it assumes the formation of a nucleus which is spontaneously generated as the result of density fluctuations in the metastable liquid phase in the form of a small vapor bubble of radius r. According to CNT, the work done to form a nucleus of radius r is given by[55]

$$W = \Delta G_v \cdot V + \gamma \cdot S = \Delta G_v \cdot \frac{4}{3}\pi r^3 + \gamma \cdot 4\pi r^2. \quad (1)$$

This equation represents the energy that must be deposited to form a bubble, which consists of two parts. The first term of Eq. (1) represents the work done on or by the system, i.e., the bulk contribution, where $\Delta G_v = G_g - G_l$ is the Gibbs energy change or free energy change per unit volume and V is the bubble volume. ΔG_v is defined as the difference between the free energy of the vapor (G_g) and liquid phase (G_l). At the boiling temperature $\Delta G_v = 0$ and the two phases are in equilibrium ($G_g = G_l$). When the temperature increases, $\Delta G_v < 0$ causing that the energy of the system decreases and a transformation from the liquid phase to the vapor phase occurs. For this reason, at elevated temperatures, the vapor phase is the most stable and has the lowest Gibbs free energy ($G_g < G_l$). The second term indicates the energy that must be deposited and stored in the surface S of the bubble, i.e., the surface contribution, where γ is surface excess energy (surface tension) per unit area.

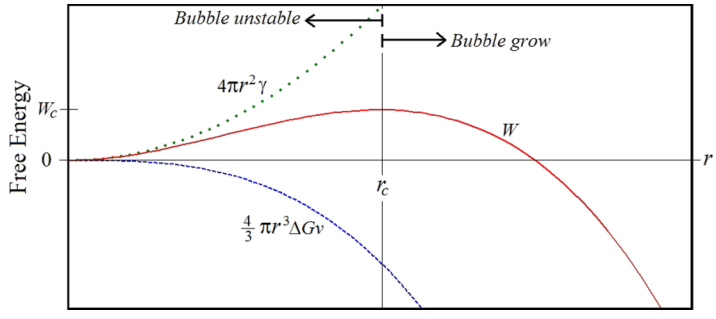

FIG. 7. Nucleation free energy as a function of the radius r. Only the bubbles larger than the critical radius r_c are stable and can grow.

Figure 7 shows the variation in energy of nucleation W with increasing size of the bubble of radius r. The CNT explains that the energy necessary to form a nucleus of radius r is the sum of the surface contribution (dotted green line) and the bulk contribution (dashed blue line). As a result, the free energy change (solid red line) exhibits a maximum value, which can be calculated under the next condition

$$\frac{\partial W}{\partial r} = 0. \tag{2}$$

Here, we can obtain the maximum value W_c for a bubble of critical radius r_c, given by

$$r_c = -\frac{2\gamma}{\Delta G_v}, \tag{3}$$

$$W_c = \frac{16}{3}\pi\frac{\gamma^3}{\Delta s G_v^2}. \tag{4}$$

The peak of the curve is the thermodynamic barrier of nucleation, which is equal to the minimum reversible work required to form a bubble of critical radius. If the radius of the bubble r is less than the critical radius r_c, the bubble is unstable and it will disappear, but once this critical radius is reached, the bubble is stable and can grow.

Most of the homogeneous nucleation theories relate W_C to the typical kinetic energy of the molecules, namely, $k_B T$ (k_B is Boltzmann's constant) and the relationship is couched in terms of the Gibbs number, $G_b = \frac{W_C}{k_B T}$. The rate of nucleation J, which determines the average number of nuclei formed in a unit volume per unit time, is related to the minimum work or by the Gibbs number in the next way

$$J = J_o \exp[-G_b], \tag{5}$$

where J_o is a factor that does not depend on the critical radius. The CNT represented by Eqs. (1) and (5) predicts the superheat limit of liquids,[56] obtaining a value of $T_{\text{cav}} = 306\,^{\circ}\text{C}$ for water at atmospheric pressure,[57] which agrees quite well with the experimental measurements reported above.

In order to explain our results on thermocavitation, we numerically solved the heat diffusion equation by finite element method with a Gaussian heat source, provided by the laser beam, given by

$$\rho C\frac{\partial T}{\partial t} + \nabla\cdot(-k\nabla T) = Q. \tag{6}$$

In the simulation, we assume as a first approximation, that none of the properties of water are affected by the addition of copper nitrate, except for its absorption coefficient. In Eq. (6), ρ is the density, C is the specific heat capacity, and k is the thermal conductivity of the water, respectively, Q is the heat source term given by $Q = \alpha I$, where α is the absorption coefficient of the solution and I is the beam's intensity. Equation (6) allows us to find the temperature at which water reaches its spinodal (~300 °C).[43–47,50,51] For such reason, in our analysis, the phase transitions water-vapor was not included, i.e., we stop the simulation once the spinodal is reached. Figure 8(a) shows that the peak temperature (~295 °C) is reached 40 ms after the laser (I_{Thr} ~16 kW/cm^2, P ~ 62 mW) is turned on, which agrees quite well with experiments. When the power is increased to 124 mW (I ~ 33 kW/cm^2), the peak temperature is higher (~332 °C) but the cavitation time shortens to $\tau_{\text{cav}} = 1.45$ ms (Figure 8(b)). Since the total bubble lifetime is just ~300 μs (for the lower power), this means that another bubble must be formed after the first cavitation occurs, i.e., bubble formation is a quasi-periodic process with frequency dependent on the beam power as noted earlier.[30] Likewise, for the case of 124 mW, the cavitations' frequency must be faster. Thus, our simulations explain why the cavitation frequency is intensity-dependent.

Figure 9 shows the superheated volume of water above 100 °C as a function of the laser power. It is clear that the superheated liquid volume is larger for low power than high power. This indicates that heat diffusion determines the water volume available for vaporization and thus the bubble size.[30] Thermal confinement is achieved when pulse length is much shorter than the heat diffusion time. In reality, true thermal confinement is never achieved since the characteristic heat diffusion time is

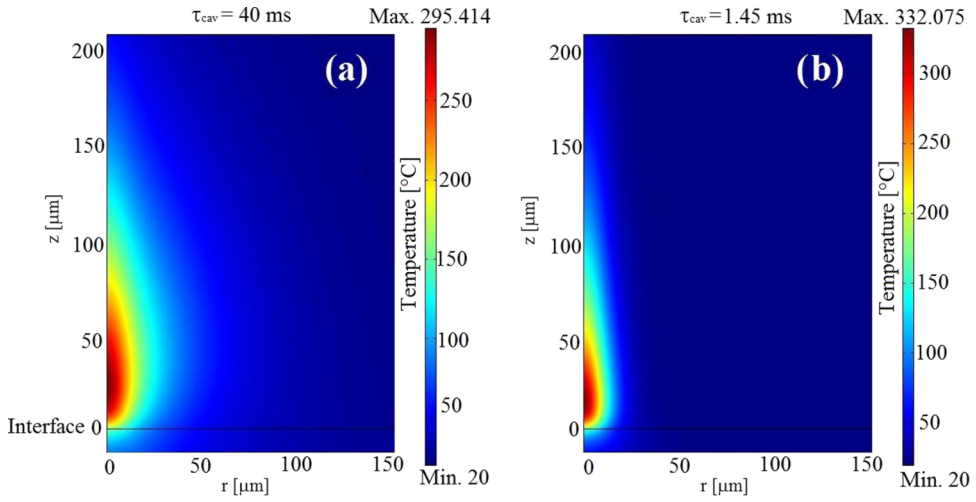

FIG. 8. Temperature profile around the focal point induced by the laser light absorption just before cavitation occurs obtained by solving the time-dependent heat transfer equation. The beam focus was placed at z=75 μm above the interface (glass-liquid). Given the symmetry of the problem and in order to minimize the computing time, only one half of the image is shown. (a) is 62 mW and (b) is 124 mW of laser power.

~2 ms (Ref. 30) and the pulse length used to generate the bubbles is comparable to this time scale. It can be seen that for a power of 62 mW, the superheated volume of water is $\sim 94 \times 10^{-5}$ mm^3 while for 124 mW, it is $\sim 18 \times 10^{-5}$ mm^3 and it decreases exponentially. Thus, numerical simulations explain most of our reported measurements.

Jitter can be understood in terms of the probability of thermocavitation within the superheated volume (see Figure 9). Let us assume that during a time τ, a superheated volume V_{sh} is achieved. Then, from Eq. (5) one ensures that $JoV_{sh}\tau_{cav} > 1$, thus the probability S of obtaining thermocavitation is[58]

$$S = 1 - exp\left[-J_o V_{sh}\tau_{cav} exp\left(-\frac{W_c}{K_b T}\right)\right]. \tag{7}$$

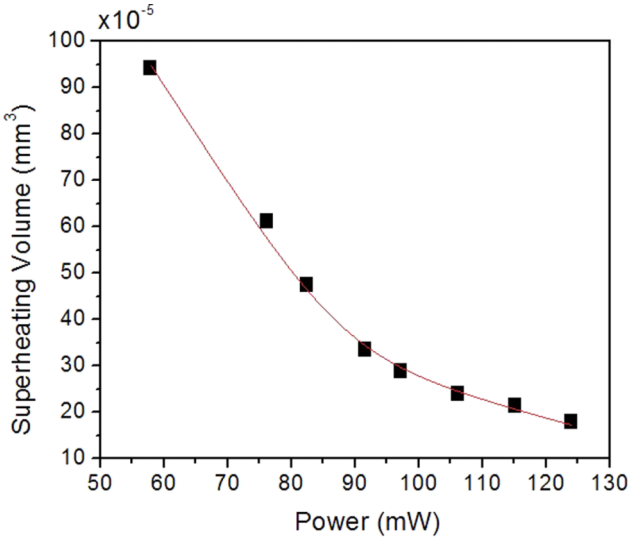

FIG. 9. Superheating volume of water (T > 100 °C) as a function of the beam power. Solid line represents a fit to an exponential decay function. Changing the beam position only changes the beam intensity at the interface since the absorption coefficient is quite large and, therefore, it changes the superheated water volume.

Therefore, thermocavitation is more likely to occur when the temperature is high but it may also occur in lower temperature regions. This gives rise to earlier or later cavitation within the same volume (see Figure 4). As mentioned above, at lower power the superheated volume is larger and, therefore, large jitter. On the contrary, larger power means smaller superheated volume, and thus smaller jitter.

VI. CONCLUSION

In this review, we showed that it is possible to generate cavitation bubbles using a CW laser focused in a saturated solution of copper nitrate, with the added advantage of an inexpensive energy source relative to other methods used for the bubble formation. The physical mechanism of bubble formation is different from that induced by pulsed lasers, ultrasound, or electrical discharger. Thermocavitation is due to the high laser light absorption by a homogeneous solution at a specific laser wavelength, which enables the focal point to reach superheated conditions (~300 °C). The superheated limit or spinodal limit coincides with the predictions of nucleation theory. At this temperature, the superheated water becomes unstable to random density fluctuations and an explosive phase transition to vapor takes place producing a fast-expanding vapor bubble. Using high speed video, we observed that thermocavitation bubbles are always attached to the solid surface taking a semi-spherical shape as they grow, in contrast to those produced by SLP.

We showed that thermocavitation can produce large cavitation bubbles by controlling the superheated water volume and we found that it is a quasi-periodic process. Our results and simulations show that, above the threshold for bubble formation, the maximum bubble radius, the cavitation time and, therefore, the shock wave amplitude, decrease exponentially with laser power. The shock waves produced by thermocavitation may be capable of producing damage to substrates, for example, in metallic, dielectric thin films, and biological substrates.

ACKNOWLEDGMENTS

The authors acknowledge financial support from CONACyT-Mexico under the project CB-2010-153463.

[1] J. R. Blake and D. C. Gibson, "Cavitation bubbles near boundaries," Annu. Rev. Fluid Mech. **19**, 99 (1987).
[2] Lord Rayleigh, "On the pressure developed in a liquid during the collapse of a spherical cavity," Philos. Mag. **34**, 94 (1917).
[3] M. S. Plesset, "Bubbles dynamics and cavitation," Annu. Rev. Fluid Mech. **9**, 145 (1977).
[4] C. E. Brennen, *Cavitation and Bubble Dynamics* (Oxford University Press, USA, 1995).
[5] J. M. Michel and J. P. Franc, *Fundamentals of Cavitation* (Springer, 2004).
[6] C.-D. Ohl, T. Kurz, R. Geisler, O. Lindau, and W. Lauterborn, "Bubbles dynamics, shock waves and sonoluminescence," Philos. Trans. R. Soc., A **357**(1751), 269 (1999).
[7] N. Korneev, P. Rodriguez-Montero, R. Ramos-Garcia, J. C. Ramirez-San-Juan, and J. P. Padilla-Martinez, "Ultrasound induced by CW laser cavitation bubbles," in *2nd International Symposium on Laser-Ultrasonics-Science, Technology and Applications* [J. Phys.: Conf. Ser. **278**, 012029 (2011)].
[8] A. Philipp and W. Lauterborn, "Cavitation erosion by single laser produced bubbles," J. Fluid Mech. **361**, 75 (1998).
[9] W. D. Song, M. H. Hong, B. Lukyanchuk, and T. C. Chong, "Laser-induced cavitation bubbles for cleaning of solid surfaces," J. Appl. Phys. **95**(6), 2952 (2004).
[10] H. Azhari, "Ultrasound: Medical imaging and beyond (an invited review)," Curr. Pharm. Biotechnol. **13**, 2104 (2012).
[11] A. J. Coleman, J. E. Saunders, L. A. Crum, and M. Dyson, "Acoustic cavitation generated by an extra corporeal shockwave lithotripter," Ultrasound Med. Biol. **13**, 69 (1987).
[12] S. J. Putterman, "Sonoluminescence: Sound into light," Sci. Am. **272**(2), 46 (1995).
[13] L. A. Crum, "Sonoluminescence," Phys. Today **47**(9), 22 (1994).
[14] *Cavitation and Inhomogeneities in Underwater Acoustics*, edited by W. Lauterborn (Springer, Berlin, Heidelberg, 1980), Vol. 4.
[15] C. B. Bucknall, A. Karpodinis, and X. C. Zhang, "A model for particle cavitation in rubber-toughened plastics," J. Mater. Sci. **29**, 3377 (1994).
[16] W. Lauterborn, "Optic cavitation," J. Phys. Colloq. **40**, C8-273 (1979).
[17] W. Lauterborn, "High-speed photography of laser-induced breakdown in liquids," Appl. Phys. Lett. **21**, 27 (1972).
[18] A. Vogel and W. Lauterborn, "Acoustic transient generation by laser-produced cavitation bubbles near solid boundaries," J. Acoust. Soc. Am. **84**(2), 719 (1988).
[19] K.-T. Byun, H.-Y. Kwak, and S. W. Karng, "Bubble evolution and radiation mechanism for laser-induced collapsing bubble in water," Jpn. J. Appl. Phys. Part 1 **43**, 6364 (2004).

[20] I. Akhatov, O. Lindau, A. Topolnikov, R. Mettin, N. Vakhitova, and W. Lauterborn, "Collapse and rebound of a laser-induced cavitation bubble," Phys. Fluids **13**, 2805 (2001).
[21] S. F. Rastopov and A. T. Sukhodolsky, "Cluster nucleation in the process of CW laser induced thermocavitation," Phys. Lett. A **149**, 229 (1990).
[22] S. F. Rastopov and A. T. Sukhodolsky, "Sound generation by thermocavitation induced CW-laser in solutions," Proc. SPIE **1440**, 127 (1991).
[23] T. Asshauer, K. Rink, and G. Delacrétaz, "Acoustic transient generation by holmium-laser-induced cavitation bubbles," J. Appl. Phys. **76**, 5007 (1994).
[24] M. Frenz, H. Pratisto, F. Konz, E. D. Jansen, A. J. Welch, and H. P. Weber, "Comparison of the effects of absorption coefficient and pulse duration of 2.12-pm and 2.79-pm radiation on laser ablation of tissue," IEEE J. Quantum Electron. **32**, 2025 (1996).
[25] K. F. Chan, G. J. Vassar, T. Joshua pfefer, J. M. H. Teichman, R. D. Glickman, S. T. Weintraub, and A. J. Welch, "Holmium:YAG laser lithotripsy: A dominant photothermal ablative mechanism with chemical decomposition of urinary calculi," Lasers Surg. Med. **25**, 22 (1999).
[26] R. S. Taylor and C. Hnatovsky, "Growth and decay dynamics of a stable microbubble produced at the end of a near-field scanning optical microscopy fiber probe," J. Appl. Phys. **95**(12), 8444 (2004).
[27] C. P. Lina and M. W. Kelly, "Cavitation and acoustic emission around laser-heated microparticles," Appl. Phys. Lett. **72**, 2800 (1998).
[28] H. W. Baac, J. G. Ok, A. Maxwell, K.-T. Lee, Y.-C. Chen, A. J. Hart, Z. Xu, E. Yoon, and L. J. Guo, "Carbon-Nanotube optoacoustic lens for focused ultrasound generation and high-precision targeted therapy," Sci. Rep. **2** (2012).
[29] J. P. Padilla-Martinez, G. Aguilar, J. C. Ramirez-San-Juan, and R. Ramos-Garcia, "Temporal evolution of thermocavitation bubbles using high speed video camera," Proc. SPIE **8097**, 809727 (2011).
[30] J. C. Ramirez-San Juan, E. Rodriguez-Aboytes, A. E. Martinez-Canton, O. Baldovino-Pantaleon, A. Robledo-Martinez, N. Korneev, and R. Ramos-Garcia, "Time-resolved analysis of cavitation induced by Cw lasers in absorbing liquids," Opt. Express **18**, 8735 (2010).
[31] A. Vogel, J. Noack, K. Nahen, D. Theisen, S. Busch, U. Parlitz, D. X. Hammer, G. D. Noojin, B. A. Rockwell, and R. Birngruber, "Energy balance of optical breakdown in water at nanosecond to femtosecond time scales," Appl. Phys. B **68**, 271 (1999).
[32] S. Fujikawa and T. Akamatsu, "Effects of the non-equilibrium condensation of vapour on the pressure wave produced by the collapse of a bubble in a liquid," J. Fluid Mech. **97**, 481 (1980).
[33] J. C. Ramirez-San-Juan, J. P. Padilla-Martinez, P. Zaca-Moran, and R. Ramos-Garcia, "Micro-hole drilling in thin films with cw low power lasers," Opt. Mater. Express **1**, 598 (2011).
[34] A. Vogel and V. Venugopalan, "Mechanisms of pulsed laser ablation of biological tissues," Chem. Rev. **103**, 577 (2003).
[35] A. P. Prishivalko, "Heating and destruction of water drops on exposure to radiation with inhomogeneous internal heat evolution," Sov. Phys. J. **26**(2), 142 (1983).
[36] J. A. De. Luc, "Introduction à la physique terrestre par les fluides expansibles," Paris: la Veuve Nyon **2**, 93 (1803).
[37] F. B. Kenrick, C. S. Gilbert, and K. L. Wismer, "The superheating of liquids," J. Phys. Chem. **28**, 1297 (1924).
[38] L. J. Briggs, "Maximum superheating of water as a measure of negative pressure," J. App. Phys. **26**, 1001 (1995).
[39] M. L. Dufour, "Sur l'ébullition des liquides," C. R. Acad. Sci. **52**, 986 (1861).
[40] G. R. Moore, "Vaporization of superheated dropsin liquids," AIChE J. **5**, 458 (1959).
[41] H. Wakhesima and K. Takata, "On the limit of superheat," J. Phys. Soc. Jpn. **13**, 1398 (1958).
[42] R. E. Apfel, "Vapor nucleation at a liquid-liquid interface," J. Chem. Phys. **54**, 62 (1971).
[43] M. Blander, D. Hengstenberg, and J. L. Katz, "Bubble nucleation in n-pentane, n-hexane, n-pentane +hexadecane mixtures, and water," J. Phys. Chem. **75**, 3613 (1971).
[44] R. E. Apfel, "Water superheated to 279. 5 ˚C at atmospheric pressure," Nat. Phys. Sci. **238**, 63 (1972).
[45] V. P. Skripov and P. A. Pavlov, "Explosive boiling of liquids and fluctuation nucleus formation," High Temp. (USSR) **8**, 782 (1970) [translated from Teplofiz. Vys. Temp., **8**, 833 (1970)].
[46] K. P. Derewnicki, "Experimental studies of heat transfer and vapour formation in fast transient boiling," Int. J. Heat Mass Transfer **28**, 2085 (1985).
[47] S. Glod, D. Poulikakos, Z. Zhao, and G. Yadigaroglu, "An investigation of microscale explosive vaporization of water on an ultrathin Pt wire," Int. J. Heat Mass Transfer **45**, 367 (2002).
[48] D. W. Oxtoby, "Homogeneous nucleation: Theory and experiment," J. Phys.: Condens. Matter **4**, 7627 (1992).
[49] H. J. Maris, "Theory of nucleation," C. R. Phys. **7**, 946 (2006).
[50] R. G. Pinnick, A. Biswas, R. L. Armstrong, S. G. Jennings, J. D. Pendleton, and G. Fernandez, "Micron-sized droplets irradiated with a pulsed CO_2 laser: Measurement of explosion and breakdown threshold," Appl. Opt. **29**, 918 (1990).
[51] S. I. Kudryashov, K. Lyon, and S. D. Allen, "Photoacoustic study of relaxation dynamics in multibubbles systems in laser-superheated water," Phys. Rev. E **73**, 055301(R) (2006).
[52] O. Yavas, P. Leiderer, H. K. Park, C. P. Grigoropoulos, C. C. Poon, W. P. Leung, N. Do, and A. C. Tam, "Optical reflectance and scattering studies of nucleation and growth of bubbles at a liquid–Solid interface induced by pulsed laser heating," Phys. Rev. Lett. **70**, 1830 (1993).
[53] F. Donny, "Mémoire sur la cohésion des liquides, et sur leur adhérence aux corps solides," Ann. Chim. Phys. **16**, 167 (1846).
[54] G. J. Brereton, R. J. Crilly, and J. R. Spears, "Nucleation in small capillary tubes," Chem. Phys. **230**, 253 (1998).
[55] W. P. Schmelzer, *Nucleation Theory and Applications* (Wiley-VCH, 2005), Vol. 76.
[56] C. T. Avedisian, "The homogeneous nucleation limits of liquids," J. Phys. Chem. Ref. Data **14**, 695 (1985).
[57] F. Caupin and E. Herbert, "Cavitation in water: Review," C. R. Phys. **7**, 1000 (2006).
[58] M. S. Pettersen, S. Balibar, and H. J. Maris, "Experimental investigation of cavitation in superfluid ^{4}He," Phys. Rev. B **49**, 12062 (1994).